A special chamber for testing electromagnetic emissions in the near field zone

Krzysztof Trzcinka
Łukasiewicz Research Network - Industrial Research Institute for Automation & Measurements PIAP
Warsaw, Poland
krzysztof.trzcinka@piap.lukasiewicz.gov.pl

Renata Markowska
Faculty of Electrical Engineering Bialystok University of Technology
Bialystok, Poland
r.markowska@pb.edu.pl

Rafał Kłoda
Łukasiewicz Research Network - Industrial Research Institute for Automation & Measurements PIAP
Warsaw, Poland
rafal.kloda@piap.lukasiewicz.gov.pl

Wiktor Pawlak
Łukasiewicz Research Network - Industrial Research Institute for Automation & Measurements PIAP
Warsaw, Poland
wiktor.pawlak@piap.lukasiewicz.gov.pl

Michał Hoinca
Łukasiewicz Research Network - Industrial Research Institute for Automation & Measurements PIAP Warsaw, Poland
MichalHoinca@outlook.com

***Abstract*— This article describes the construction of a test stand for locating disturbance sources using an EMC scanner placed in a dedicated EMC test chamber. Special attention was paid to the EMC test chamber and the solutions used for shielding and minimizing reflections of electromagnetic waves inside the chamber. The research results presented in this article concern the influence of the chamber construction on the possibility of locating the source of disturbances. Mainly, the results obtained when only shielding materials were used in the chamber to eliminate background disturbances of the environment and when ferrite plates were additionally installed on the walls were compared. The obtained test results in the chamber with ferrite plates on the walls are satisfactory.**

Keywords*— *EMC test chamber, EMC scanner, near-field probes, location of sources of electromagnetic disturbances, radiated emission.

I. INTRODUCTION

Electromagnetic compatibility (EMC) is an important aspect ensuring the possibility of simultaneous reliable operation of many devices in a given electromagnetic environment. The devices should not emit disturbances with too high levels exceeding the limits of the standards and at the same time should be immune to electromagnetic disturbances in the surrounding environment [1]. Each device placed on the market in accordance with the EMC Directive must meet specific technical requirements in the field of electromagnetic compatibility, which should be confirmed by a positive result in the test report.

This article describes the issue of radiated electromagnetic emission measurements for mobile robots. A test stand with a specialized chamber for EMC testing was proposed. The test stand can be used at the stage of identifying the source that causes too high levels of electromagnetic disturbance emission in the device that obtained a negative test result.

Mobile robots produced by Łukasiewicz-PIAP Institute are devices that use the latest technologies. These are battery-powered devices, consisting of a mobile base and a control console, see Fig. 1. Communication between the console and the mobile base is carried out using radio waves or via a fiber optic link. The mobile base of such a robot is its executive element consisting of a wheel or wheel-caterpillar drive, equipped with cameras and microphones with the possibility of mounting accessories such as a manipulator, a set of observation cameras and other specialized devices and sensors. In turn, the control console is equipped with a high-resolution screen and control elements such as joysticks, buttons, etc. It is used to remotely control the robot and to receive and record data collected by the robot's sensors. Such robots are used to recognize the terrain and hard-to-reach places and to remove dangerous loads/devices. They are used by various services such as: border guards, police and army.

Fig. 1. PIAP GRYF® mobile robot, mobile base on the left, control console on the right.

However, the most demanding user of robots is the army, hence the requirements for them are very strict. Therefore, developing a mobile robot design and implementing it for use

in the armed forces is a very complicated, expensive and time-consuming process. First of all, the robot must meet strict functional requirements, hence its design must be adapted to the specific requirements of the order. Moreover, it must also meet very strict requirements of military standards, including EMC requirements. The EMC requirements for mobile robots (battery-powered devices) are presented in the military standard NO-06-A200:2012 [2] and concern the requirements of immunity to electromagnetic fields and the requirements of radiated emission.

II. RESEARCH PROBLEM

In the case of delivery of a mobile robot for the army, it is usually a new product that must be adapted to military functional requirements and the requirements of military standards. The developed mobile robot prototype must pass a series of acceptance tests, including EMC tests, which are among the most demanding. A negative result of one of the tests may cause problems for the manufacturer, because contractual penalties under the contract can be very high. It should be emphasized that the EMC tests for such a robot are quite demanding. The more difficult they are to pass, because the mobile robot is packed with new technologies and is equipped with various sensors. This makes obtaining the positive EMC test result of a prototype of such a device not an easy task for engineers, especially within radiated emission measurements. This is also because the limit allowed for military land devices in the range from 2 MHz to 18 GHz is very low, e.g. in the range from 2 MHz to 100 MHz the limit is 24 dBμV/m measured at a distance of 1 m (see Fig. 2).

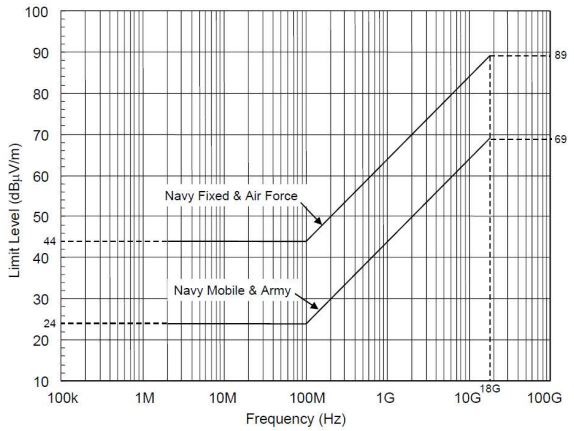

Fig. 2. Radiated emission limit used for mobile robots - Navy Mobile & Army limit line [3].

The complexity of the construction of the mobile robot base and the robot control console, including the need to use new construction materials such as composites and other technical requirements make the implementation of tight electromagnetic shielding of such a device quite expensive and very difficult to implement. This may have a negative impact on the final result of radiated emission tests.

Therefore, tools and methods are sought that will allow for quick initial engineering tests of radiated emission, so as to identify and locate sources of excessive radiated disturbances as soon as possible, in order to eliminate them and obtain a positive emission test result. The more so because in the case of mobile robots delivered to the armed forces, the deadlines for implementation are very short, which is why the tools and methods used should be effective and quick to implement.

Methods of searching for sources of disturbances using near-field probes, where an engineer equipped with a spectrum analyzer and a set of near-field probes tries to identify places with the highest level of radiated emission, have been available and known for a long time [4, 5]. There are also other methods of identifying the places of electromagnetic leakage, consisting in disconnecting the elements or circuits of the device for the duration of the measurement and comparing the obtained results with the reference measurement, i.e. when the device was tested in its full configuration and the measurements were performed in accordance with standardized methods in the SAC chamber [6].

Examples from the literature include also the use of the EMSCAN tool, i.e. a near-field scanner with stationary probes, which together with to the methodology of manual positioning of near-field probes, was used to identify the source of disturbances arosing after changing the topology of electronic components in the car converter [7]. The process of identifying the source of disturbances consisted in performing a measurement in the SAC chamber using a standardized method and determining the frequencies at which the limit and exceedances occur, and then using the EMSCAN scanner to identify the places and elements being the sources of emission observed during measurements inside the SAC chamber. Thanks to this method, the sources of disturbances were identified, but the tested device was a small PCB of a DC-DC converter with electronic components without a housing. The authors praise that thanks to the EMSCAN tool, it was possible to find the source of the disturbance and remove the problem.

Other methods of measuring the intensity of the electromagnetic field in the near zone, described in the literature, allow to identify the sources of undesirable emission [8], but for simple objects such as a printed circuit board [9], [10], [11], for integrated circuits [12] or for simple devices with small dimensions [13].

To measure radiated emissions in the near zone, a spectrum analyzer and a set of near field probes are required. There are also commercially available entire stands for automatic performance of such measurements, the so-called EMC scanners, e.g. a scanner from Detectus [14]. However these are devices applicable to printed circuit boards (PCBs) and small devices and do not provide the possibility of testing large-sized and complex devices, such as mobile robots.

III. EMC TEST STAND

A. EMC scanner

Initial experience with measurements of radiated emission in the near-field zone of mobile robots using the method with manual positioning of near-field probes did not give satisfactory results, among others due to disturbances interfering with the measurements from the ambient background and due to low repeatability [5]. In addition, the analysis of cases from the literature includes a number of

different methods and solutions, which, however, according to the authors, still require further research and improvement. Therefore, using the practical experience gained and knowledge from the literature, it was decided to build a dedicated test stand to locate the sources of electromagnetic emission disturbances in the prototypes of mobile robots.

Hence, the concept of building an EMC scanner was born, which, by means of electromagnetic field strength measurements in the near field zone, will enable the location of disturbance sources in mobile robots manufactured by Łukasiewicz-PIAP, sources of disturbances that cause a negative radiated emission test result. It was assumed that the testing stand will be used in the frequency range from 30 MHz to 1 GHz and will allow testing of devices with maximum dimensions of 1200 x 900 x 600 mm, corresponding to mobile robots manufactured by Łukasiewicz-PIAP. The construction concept of the EMC scanner is shown in Fig. 3, where its main components are listed.

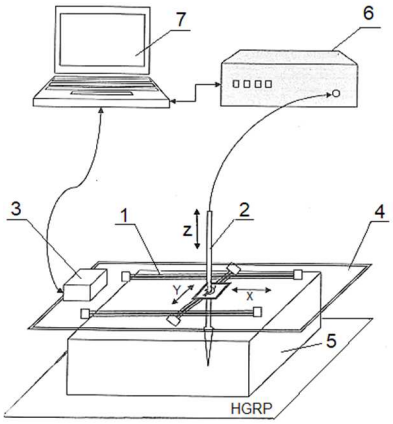

Where:
1. XY Cartesian robot.
2. Z axis EM field probe (manual setting).
3. XY robot power supplies and motor drivers.
4. Supporting structure for the robot.
5. Measuring space for the tested EUT device.
6. Spectrum analyzer.
7. Computer with XY robot control software and spectrum analyzer.

Fig. 3. The construction concept of the EMC scanner with the automatic positioning of the measuring probe.

The EMC scanner (fig. 3) is a measuring device using a spectrum analyzer connected to a near-field probe, which is positioned automatically in a flat measuring space, the vertical axis is set manually. The computer controls the measurement process, positions the near-field probe, and collects and visualizes the measurement data.

Preliminary measurements of near field radiated emission using the developed EMC scanner and the classical method with manual positioning of near field probes revealed that keeping low level of the external electromagnetic field strength and ensuring repeatability of measurements might be crucial for successful locating the sources of disturbances within the device. Therefore it was decided to develop and build a specialized chamber for conducting electromagnetic field strength measurements in the near-field zone using the EMC scanner. The construction of the chamber included shielding materials and ferrite plates. The study presented in the article concentrate on assessing the influence of the chamber construction on the effectiveness of locating the source of disturbances within EUT.

B. Specilized chamber for the near field radiated emission tests

The concept of a specialized chamber for EMC tests involves building a shielded room with dimensions adapted to the EMC scanner to limit disturbances from the external environment. In addition, it was planned to cover the inner walls of the chamber with ferrite absorbers to minimize the reflections of electromagnetic waves from the metal walls. The operating frequency range of the chamber is from 30 MHz to 1 GHz. During the design of the chamber, it was planned to perform tests and measurements at various stages of its implementation, i.e. after installing a metal cage shielding from external electromagnetic fields (see Fig. 5) and additionally, after lining the cage's walls with ferrite plates.

The concept of construction of a specialized EMC test chamber is shown in fig. 4. It can be seen that it is a self-supporting structure, made of wooden elements with two mobile doors installed on opposite walls.

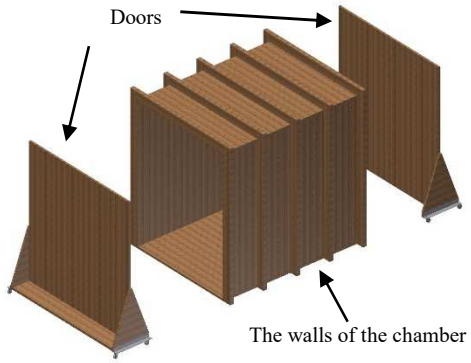

Fig. 4. The concept of building a specialized EMC test chamber.

Aluminum foil with a width of 1 m and a thickness of 0.1 mm was used as the shielding material for the chamber, and additionally a T217 type shielding wallpaper was used as the second layer of the screen [15]. The shield made in this way was placed on the outside of the chamber structure (fig. 6). The internal walls of the chamber, floor and ceiling were covered with ferrite tiles measuring 100 x 100 mm.

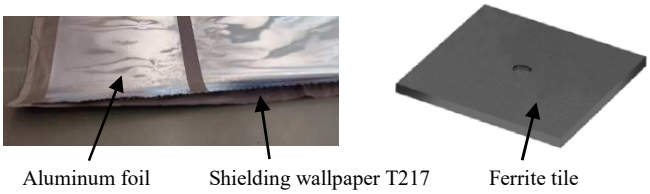

Fig. 5. Elements used to build the chamber. On the left, a view of the double-layer shield of the chamber (aluminum foil and shielding wallpaper), on the right, the absorber - ferrite tile (20 MHz - 1000 MHz).

Wooden beams with dimensions of 100 x 100 mm and 100 x 50 mm were used as the supporting structure of the chamber, while the walls were made of MDF boards with appropriately prepared holes for the installation of ferrite plates. The chamber is equipped with two doors on wheels as self-supporting structures. Thanks to this, the chamber is mobile, it can be moved on a typical forklift. The internal dimensions of the

chamber are 1500 x 2020 x 1805 mm [W x L x H]. The view of the construction of the chamber and the door is shown in Fig. 6.

Fig. 6. View of the construction of the EMC test chamber with an external metallic shield installed (the chamber during its construction) and the door of chamber on the right.

On one of the side walls, a feed-through panel was installed with coaxial connectors for measurement signals from near-field measuring probes and with connectors for outputting measurement and control signals from the EMC scanner located inside the chamber. The view of the complete chamber is shown in Fig.7. The view of the internal walls and the inside of the door after installing the ferrite plates is shown in Fig. 8.

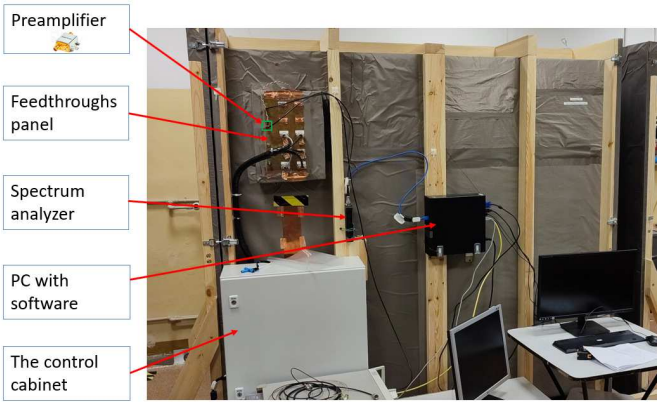

Fig. 7. View of the specialized EMC chamber from the outside, from the side of the feed-through panel.

After the construction of the specialized chamber for EMC testing was completed, measurements of the background level of disturbances inside the chamber were carried out. The graph in Fig. 9 shows the level of electromagnetic field strength measured with the chamber door open (red line) and the level of electromagnetic field strength with the door closed (dark blue) measured with the near-field probe (E-field probe, type 904 - see Fig. 12 a). The E-field probe (omnidirectional) was placed in the central point of the chamber at a height of 80 cm from the floor. The presented measurement results show that the shielding properties of the chamber ensure a low level of background disturbances, for example, for the frequency of 100MHz, the difference in the background level of disturbances with the chamber door open and closed is about 33 dB.

Fig. 8. View of the specialized EMC chamber inside, after filling the walls and doors with ferrite plates. On the left inside the chamber one can see the construction of the EMC scanner.

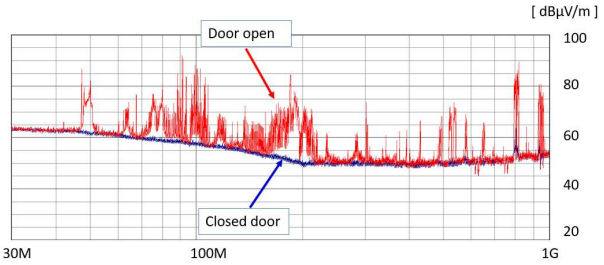

Fig. 9. Results of measurements of background disturbances in the chamber when the door was open and when the door was closed.

IV. METHODOLOGY AND RESEARCH RESULTS

To test the measurement and research properties of the stand with the EMC scanner installed inside the chamber, i.e. the possibility of locating sources of electromagnetic disturbances by visualizing the distribution of electromagnetic field strength in a horizontal plane, the setup of the stand shown in Fig. 10 was used. In the measurement area inside the specialized chamber for EMC tests, a fictitious source of electromagnetic disturbances was placed. The disturbance source was simulated by a PCB with a straight path 200 mm long and 1 mm wide (fig. 11) powered from an external signal generator.

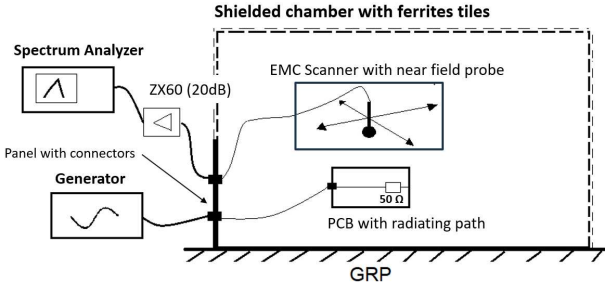

Fig. 10. Block diagram of the test setup with EMC scanner and EMC chamber.

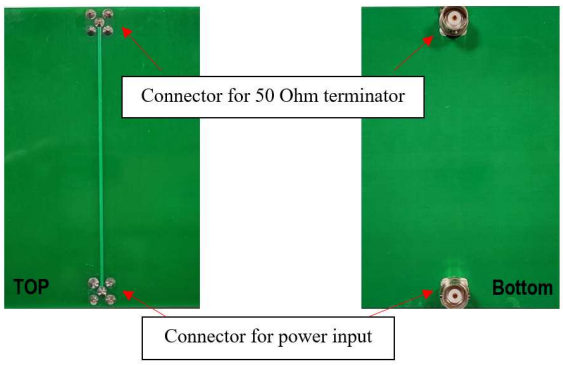

Fig. 11. Radiating path (200 mm long and 1 mm wide) that simulates a disturbance source powered by a generator.

The source of disturbances prepared in this way with known parameters (dimensions and shape, frequency and amplitude of the signal) was subjected to measurements of the electromagnetic field strength distribution using the EMC scanner in a horizontal plane at a distance of 10 mm above the PCB (Spectrum Analyzer settings: PEAK detector, RBW = 100kHz). Measurements were made with a step of moving the probe every 10 mm. In each analyzed case an area of the environment larger than the surface of the PCB was scanned (area extending to 4÷6 cm from each edge of the PCB). Measurements were made with a ball-type electric field (E) probe (Fig. 12a), and then with a loop-type magnetic field (H) probe (Fig. 12b) for different polarizations of the field: Hy - when the loop of the probe was positioned in the plane parallel to the radiating path (vertically), and Hx - when the probe loop was positioned in the plane perpendicular to the path.

Fig. 12. Near-field probes (ETS-LINDGREN model 7405) used for measurements: a) Type 904 probe, E field, 3 cm ball (omnidirectional), b) Type 902 probe, H field, 3 cm loop.

After taking and archiving a series of measurements in the shielded chamber, the inner walls of the chamber were covered with ferrite plates and the same series of measurements was made again, for the same configuration. Fig. 13 below shows the scanned area of the PCB and the scanned space protruding beyond the PCB area. It is a graph of the color map, changing depending on the value of the measured signal level, in such a way that the highest signal level in the visualization is red and the lowest green. The graph corresponds to the amplitudes of the spectrum of the electromagnetic field strength, the E component, measured with the E-field probe. On the obtained color map of the scanned area, the area of the scanned PCB and the location of the radiating path are marked.

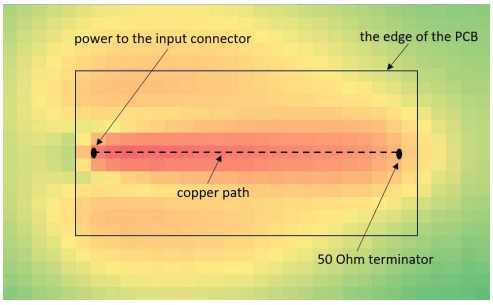

Fig. 13. Spatial distribution of the electric component of the electromagnetic field strength over a PCB with a radiating path 200mm long and 1mm wide. Measurements in the chamber with walls covered with ferrite plates. The measurements were made with a ball-type E-field probe at a distance of 1 cm from the scanned PCB. The frequency of the signal supplying the radiating path was 200 MHz.

Further studies were carried out in such a way that the scanning of the PCB with the radiating path was performed with the ball E-field probe (type 904) for three different frequencies of the signal supplying the radiating path: 200MHz, 400MHz and 600MHz at a constant signal level of 0 dBm, and then these measurements were repeated with the loop H-field probe (loop with a diameter of ϕ= 3 cm, type 902). The graphs below were obtained based on the measured amplitudes of the electromagnetic field strength spectrum, the E component in Fig. 14 and 15 and the H component in Fig. 16 ÷ 19. Measurements were made in the shielded chamber before the installation of ferrite tiles (Fig. 14, 16 and 18) and repeated after the ferrite tiles installation (Fig. 15, 17 and 19).

A. Measurements of the electric field strength

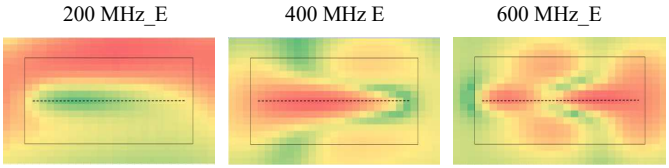

Fig. 14. Spatial distribution of the electric component of the electromagnetic field strength above the PCB with the radiating path (200 mm long and 1 mm wide). Measurements were made in the shielded chamber with metal walls using a ball E-field probe (type 904) at the frequencies of 200 MHz, 400 MHz and 600 MHz at a distance of 1cm from the scanned PCB.

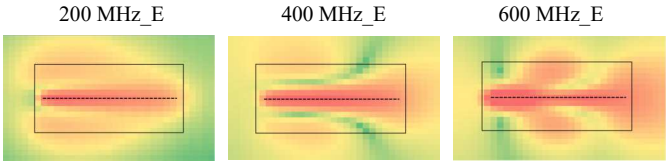

Fig. 15. Spatial distribution of the electric component of the electromagnetic field strength above the PCB with the radiating path (200 mm long and 1 mm wide). Measurements were made in a chamber with walls covered with ferrite plates using a ball E-field probe, at the frequencies of 200 MHz, 400 MHz and 600 MHz, at a distance of 1cm from the scanned PCB.

Table I below presents the comparison of the maximum values of the amplitudes of the electric component of the electromagnetic field strength, corresponding to the measurement results presented in Fig. 14 and Fig. 15.

TABLE I. MAXIMUM AMPLITUDES OF THE ELECTRIC COMPONENT OF THE ELECTROMAGNETIC FIELD STRENGTH, MEASURED DURING THE SCANNING OF THE PCB IN THE SHIELDED CHAMBER BEFORE AND AFTER THE INSTALLATION OF THE FERRITE PLATES.

f [MHz]	E_s	E_f	$E_s - E_f$
	[dBμV/m]		
200	115,6	102,6	13
400	117,1	110,7	6,4
600	115,8	112,3	3,5

Where: E_s and E_f are the maximum amplitudes of the electric component of the electromagnetic field strength measured while scanning the PCB with the electric field probe E, ball type 904.
E_s – means the measurement made in the shielded chamber without ferrite plates,
E_f – means the measurement made in the shielded chamber with ferrite plates on the walls.

From the measurements of the spatial distribution of the E component of the electromagnetic field strength above the radiating path, carried out in the shielded chamber and in the anechoic chamber (with ferrite plates), it can be concluded that the use of ferrite plates on the walls brings good results, because distortions of the field strength above the path in the case of the chamber with ferrites are much smaller than for measurements in the shielded chamber with metal walls. In case of the anechoic chamber the maximum field strength amplitudes marked in red imitate the image of the radiating path much better than in case of the shielded chamber, especially at lower frequencies. When comparing the maximum amplitudes the electric component of the electromagnetic field strength, it was found that higher amplitudes were obtained in the case of the shielded chamber, but at the expense of the occurring field distortions, most likely caused by reflections of electromagnetic waves.

B. Measurements of the magnetic field strength

Measurements of the magnetic component H of the electromagnetic field strength above the PCB made with the H-field probe (loop with a diameter of $\phi = 3$ cm, type 902) at the Y polarization (the probe loop positioned in the plane parallel to the radiating path) are shown in Fig. 16 and Fig. 17 for three different frequencies 200 MHz, 400 MHz and 600 MHz.

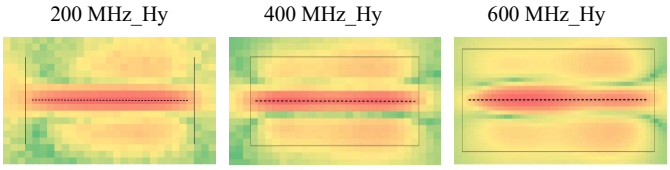

Fig. 16. Spatial distribution of the magnetic component of the electromagnetic field strength at a distance of 1 cm above the radiating path (200 mm long and 1 mm wide). Measurements made in the shielded chamber with metal walls using the H field probe at the Y polarization (probe loop positioned in the plane parallel to the radiating path).

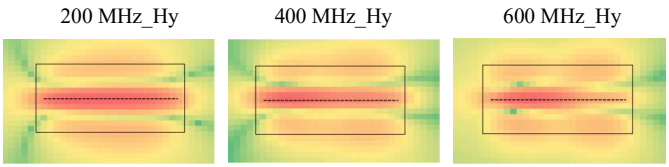

Fig. 17. Spatial distribution of the magnetic component of the electromagnetic field strength at a distance of 1 cm above the radiating path (200 mm long and 1 mm wide). Measurements made in the anechoic chamber with walls covered in ferrite plates using the H field probe at the Y polarization (probe loop positioned in the plane parallel to the radiating path).

The results of measurements of the magnetic component H of the electromagnetic field strength over the PCB for the X polarization (probe set perpendicular to the radiating path) are shown in Fig. 18 and Fig. 19.

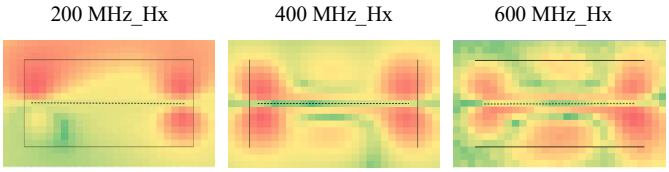

Fig. 18. Spatial distribution of the magnetic component of the electromagnetic field strength at a distance of 1 cm above the radiating path (200 mm long and 1 mm wide). Measurements made in the shielded chamber with metal walls using the H field probe at the X polarization (probe loop positioned in the plane perpendicular to the radiating path).

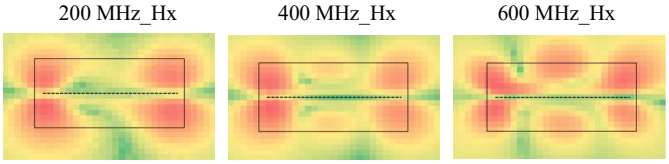

Fig. 19. Spatial distribution of the magnetic component of the electromagnetic field strength at a distance of 1 cm above the radiating path (200 mm long and 1 mm wide). Measurements made in the anechoic chamber with walls covered in ferrite plates using the H field probe at the X polarization (probe loop positioned in the plane perpendicular to the radiating path).

Table II below presents the comparison of the maximum values of the amplitudes of the magnetic component of the electromagnetic field strength, corresponding to the measurement results shown in Fig. 16 and Fig. 17. Accordingly, Table III presents the data corresponding to the measurement results shown in Fig. 18 and Fig. 19.

TABLE II. MAXIMUM AMPLITUDES OF THE MAGNETIC COMPONENT OF THE ELECTROMAGNETIC FIELD STRENGTH MEASURED AT THE Y POLARIZATION OF THE LOOP PROBE DURING THE SCANNING OF THE PCB IN THE SHIELDED CHAMBER BEFORE AND AFTER THE INSTALLATION OF THE FERRITE PLATES.

f [MHz]	$\mathbf{H_{ys}}$	$\mathbf{H_{yf}}$	$\mathbf{H_{ys} - H_{yf}}$
	[dBμA/m]		
200	61,2	75,2	-14
400	64,1	72,6	-8,5
600	62,6	66,5	-3,9

Where: $\mathbf{H_{ys}}$ and $\mathbf{H_{yf}}$ are the maximum amplitudes of the magnetic component H of the electromagnetic field strength measured when scanning the PCB with the H-field probe (3cm loop, type 902) in Y polarization, when the probe loop was positioned along the radiating path.
$\mathbf{H_{ys}}$ – means the measurement made in the shielded chamber without ferrite plates.
$\mathbf{H_{yf}}$ - means the measurement made in the shielded chamber with ferrite plates on the walls.

TABLE III. MAXIMUM AMPLITUDES OF THE MAGNETIC COMPONENT OF THE ELECTROMAGNETIC FIELD STRENGTH MEASURED AT THE X POLARIZATION OF THE LOOP PROBE DURING THE SCANNING OF THE PCB IN THE SHIELDED CHAMBER BEFORE AND AFTER THE INSTALLATION OF THE FERRITE PLATES.

f [MHz]	$\mathbf{H_{xs}}$	$\mathbf{H_{xf}}$	$\mathbf{H_{xs} – H_{xf}}$
	[dBμA/m]		
200	48,7	63,3	-14,6
400	53,1	62,7	-9,6
600	50,8	52,8	-2

Where: $\mathbf{H_{xs}}$ and $\mathbf{H_{xf}}$ are the maximum amplitudes of the magnetic component H of the electromagnetic field strength measured while scanning the PCB with the H-field probe (3cm loop, type 902) in the X polarization, when the probe loop was perpendicular to the radiating path.
$\mathbf{H_{xs}}$ – means the measurement made in the shielded chamber without ferrite plates.
$\mathbf{H_{xf}}$ – means the measurement made in the shielded chamber with ferrite plates on the walls.

From the measurements of the spatial distribution of the magnetic component H of the electromagnetic field strength above the PCB with the radiating path, carried out in the shielded chamber and in the anechoic chamber (with walls covered with ferrites), it can be concluded that:

- The results of measurements of the magnetic field strength H with Y polarization (with the probe loop positioned along the radiating path), both in the shielded chamber and in the chamber with ferrite plates, faithfully reproduce the shape of the radiating path on the PCB, however, the maximum values of the measured signal in the chamber with ferrites are higher than in the shielded chamber.

- The results of measurements of the magnetic field strength H with X polarization (with the probe loop perpendicular to the radiating path) differ for the shielded chamber and the chamber with ferrite plates. Measurement results for Hx polarization give information about the beginning and end of the radiating path. In the shielded chamber, especially for 200 MHz frequency, large distortions of the magnetic field strength can be observed. The higher the frequency of the signal supplied to the radiating path, the smaller the differences between the measurements made in the shielded chamber and in the chamber with ferrites. The maximum values of the signals in the chamber with ferrites are higher than in the shielded chamber.

C. Summary of the results of scanning the PCB with the radiating path

The measurements of the distribution of the amplitudes of the electric and magnetic field strength components above the PCB with radiating path show that the use of ferrite plates inside the chamber minimizes distortions of the spatial distribution of the field strength above the radiating path. The measurement results are more stable, they fluctuate less, which also improves the repeatability of measurements. On the basis of the obtained spatial distributions of the field strength in the chamber with ferrites, it is possible to easily locate a source of disturbances.

V. CONCLUSIONS

As can be seen from the measurements, the shielded chamber with ferrite plates meets the shielding requirements well, which ensures sufficient isolation of the measurement environment from environmental disturbances. The use of the EMC scanner in the chamber with ferrite plates is a good solution for searching (locating) sources of maximum emission (places of electromagnetic radiation leakage from the tested device), which is shown by the obtained test results. The use of ferrite plates on the inner walls of the chamber prevents distortions of the electromagnetic field, improves the repeatability of tests and is a promising tool in combination with the EMC scanner for locating sources of disturbances.

In order to draw more conclusions and fully assess the usefulness of the developed EMC test stand for locating the disturbances emitted by mobile robots, it is necessary to perform more research and analyzes. However, it should be emphasized that the preliminary results obtained are very promising.

ACKNOWLEDGMENT

The article was created as part of the "Implementation Doctorate" program of the Minister of Science and Higher Education. The implementation doctorate is carried out in cooperation with the Łukasiewicz Research Network - Industrial Institute of Automation and Measurements PIAP and the Faculty of Electrical Engineering of the Białystok University of Technology.

REFERENCES

[1] Directive 2014/30/EU of the European Parliament and of the Council of 26 February 2014 on the harmonisation of the laws of the Member States relating to electromagnetic compatibility (recast).

[2] NO-06-A200:2012 „Kompatybilność elektromagnetyczna. Poziomy dopuszczalne emisji ubocznych i odporności na narażenia elektromagnetyczne”

[3] MIL-STD-461F 10 December 2007 “REQUIREMENTS FOR THE CONTROL OF ELECTROMAGNETIC INTERFERENCE CHARACTERISTICS OF SUBSYSTEMS AND EQUIPMENT”

[4] Three techniques guide radiated-emission sources, September 30, 1999 by Dave Sangston, Motorola Computer Group

[5] Near-Field Methods of Locating EMI Sources, Vladimir Kraz Credence Technologies, Inc. 3601-A Caldwell Dr., Soquel CA 95073 USA, 1995

[6] Przesmycki, R., Wnuk, M. (2014). Metoda pomiaru wycieków elektromagnetycznych w oparciu o emisję promieniowaną jednostek centralnych PC. Przegląd Elektrotechniczny. doi:10.12915/pe.2014.07.56

[7] A. Silaghi, R. Aipu, A. De Sabata and P. Nicolae, "Near-field scan technique for reducing radiated emissions in automotive EMC," 2018 IEEE International Symposium on Electromagnetic Compatibility and 2018 IEEE Asia-Pacific Symposium on Electromagnetic Compatibility (EMC/APEMC), 2018, pp. 831-836, doi: 10.1109/ISEMC.2018.8393897.

[8] K. See et al., "An Empirical Approach to Develop Near-Field Limit for Radiated-Emission Compliance Check," in IEEE Transactions on Electromagnetic Compatibility, vol. 56, no. 3, pp. 691-698, June 2014, doi: 10.1109/TEMC.2014.2302003.

[9] D. W. P. Thomas et al., "Near-field scanning of stochastic fields considering reduction of complexity," 2017 International Symposium on Electromagnetic Compatibility - EMC EUROPE, Angers, 2017, pp. 1-6, doi: 10.1109/EMCEurope.2017.8094766.

[10] P. Maheshwari, H. Kajbaf, V. V. Khilkevich and D. Pommerenke, "Emission Source Microscopy Technique for EMI Source Localization," in IEEE Transactions on Electromagnetic Compatibility, vol. 58, no. 3, pp. 729-737, June 2016, doi: 10.1109/TEMC.2016.2524594.

[11] L. Beghou, B. Liu, L. Pichon and F. Costa, "Synthesis of Equivalent 3-D Models from Near Field Measurements— Application to the EMC of Power Printed Circuit Boards," in IEEE Transactions on Magnetics, vol. 45, no.3, pp. 1650-1653, March 2009, doi:10.1109/TMAG.2009.2012767

[12] Z. Yu, J. A. Mix, S. Sajuyigbe, K. P. Slattery and J. Fan, "An Improved Dipole-Moment Model Based on Near-Field Scanning for Characterizing Near-Field Coupling and Far-Field Radiation From an IC," in IEEE Transactions on Electromagnetic Compatibility, vol. 55, no. 1, pp. 97-108, Feb. 2013, doi: 10.1109/TEMC.2012.2207726.

[13] D. Mandaris et al., "Different Test Site Analysis of Radiated Field Measurements of a Complex EUT," 2019 International Symposium on Electromagnetic Compatibility - EMC EUROPE, Barcelona, Spain, 2019, pp. 674-679, doi: 10.1109/EMCEurope.2019.8872051.

[14] http://astat-emc.pl/produkty/urzadzenia-pomiarowe/skaner-emc/

[15] https://astat-emc.pl/wp-content/uploads/astat_dt_tapeta-ekranujaca-t217.pdf